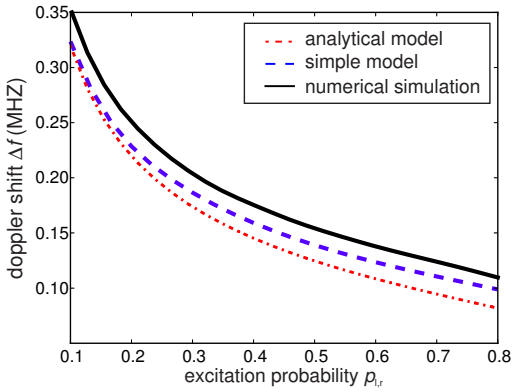

Supplementary Figure 1: Probe frequency dependent Doppler shift versus mean excitation probability $p_{\mathrm{l,r}}$: Black solid line shows the shift as determined by two point sampling from full numerical solution to master equation (1), including 8 atomic levels using the parameters of the absolute frequency measurements. Blue dashed line shows the approximate formula (11) from the 1D model neglecting diffusion. Red dash-dotted line shows the result from the analytical formula in Eq. (10). The analytical formulas are correct up to second order in the Lamb-Dicke factor, which is consistent with the discrepancy from the numerical solution.

Supplementary Note 1

Systematic shifts

There are several effects that can introduce systematic shifts to the investigated transition.

Lineshape asymmetries can be introduced through an excitation imbalance of Zeeman-shifted line components arising from imbalanced σ^+/σ^- polarization of the nominally linearly polarized spectroscopy and repump lasers. Such an asymmetry would result in a magnetic field dependent shift of the line center. We have measured the line center for three different magnetic fields (0.387(2) mT, 0.584(1) mT and 0.779(3) mT) using the two-point sampling technique. A linear fit gives a shift of -8 kHz for a magnetic field of 0.584 mT, at which the frequency measurements where performed. The uncertainty of 59 kHz is given by the 68.3% prediction bound of the fit, compatible with no shift. This uncertainty is limited by the number of measurements performed.

AC Stark shifts of the transition frequency arise from differential off-resonant coupling of electromagnetic radiation to the two involved spectroscopy states. We have investigated shifts arising from the spectroscopy laser by varying its power while simultaneously adjusting the number of spectroscopy pulses to keep the excitation signal similar. From the intensity calibration curves similar to the ones shown in Fig. 3b of the main text, the corresponding Rabi frequencies of the spectroscopy laser have been determined to be $\Omega = 2\pi\times(4.3, 5.6, 7.3)$ MHz. The center frequencies for different Rabi frequencies are evaluated using

the two-point sampling technique. A linear fit to the center frequency gives a shift of 60 kHz (with an uncertainty of 44 kHz given by the 68.3% prediction bound of the fit) for the Rabi frequency of $\Omega = 2\pi\times5.6$ MHz chosen for the frequency measurements. Possible ac Stark shifts from the repump laser pulse are eliminated by applying it after the spectroscopy laser pulse. Additional ac Stark shifts can arise from the trapping rf field if the ion is not located at the node of the radial electric quadrupole. Using a two-ion crystal in a linear Paul trap, we have minimized this effect through micromotion compensation [50] to an estimated shift of less than 1 kHz.

For the frequency measurements, we use 125 ns short spectroscopy pulses that are generated by applying rf pulses centered around 413 MHz to an acousto-optic modulator (AOM). The pulse bandwidth of ~ 8 MHz together with the limited spectral bandwidth of the AOM causes a shift of the envelope of the train of spectroscopy pulses, if the center frequencies are not matched or the AOM transfer function is asymmetric with respect to its center frequency. We measure this shift for each experimental run to within 15 kHz by performing a beat measurement between the light incident onto the AOM and the first diffraction order used for spectroscopy with a fast calibrated photodetector. A similar shift arising from the photodiode is calibrated to be 22(3) kHz. The measured shifts are applied to each frequency measurement.

Detuning-dependent Doppler shifts give rise to an asymmetry of the excitation line profile. Since we are starting in the motional ground state and the excitation signal is proportional to the ion's motion in this mode, we can accurately model this shift by either using an analytical model, or numerical simulations of the full master equation. Both are described in more detail in the next sections. The main result is shown in Supplementary Fig. 1, where we compare the shifts predicted by two analytical models and the numerical simulation implementing the full 8-level atomic system. From the numerical simulations and a conservatively estimated fluctuation of the detection signal of ±0.1, we account for a shift of 151(20) kHz.

Supplementary Note 2

Probe frequency dependent Doppler shift

We derive the probe frequency dependent Doppler shift on the basis of the following simple model. We treat the $^2S_{1/2} \leftrightarrow {}^2P_{1/2}$ transition in the spectroscopy ion as a two level transition with linewidth Γ, and we restrict the description to the selected normal mode of the two-ion crystal. During each pulse the system evolves according to

$$\dot{\rho} = -i\left[\omega_{\mathrm{m}} a^\dagger a - \frac{\Delta}{2}\sigma_z + \frac{\Omega}{2}\left(\sigma^+ e^{i\eta(a+a^\dagger)} + \mathrm{h.c.}\right), \rho\right] + \frac{\Gamma}{2}\mathcal{D}[\sigma^-]\rho, \tag{1}$$

where $\mathcal{D}[\sigma^-]\rho = (2\sigma^-\rho\sigma^+ - \sigma^+\sigma^-\rho - \rho\sigma^+\sigma^-)$, and σ^+, σ^- are the atomic raising and lowering opera-

tors, respectively, σ_z is a Pauli matrix, and $a^\dagger$ is the creation operator of the selected normal mode. In order to describe drift and diffusion of the normal mode we change to a Wigner function representation by introducing

$$w(x,p) = \frac{1}{\pi}\int \mathrm{d}y \langle x+y|\rho|x-y\rangle e^{-2iyp}$$

such that the Wigner function for the normal mode is given by the trace over the internal degrees of freedom, $W(x,p) = \mathrm{tr}_{\mathrm{int}}\{w(x,p)\}$. In the Wigner function representation we can apply the replacement rules

$$e^{\pm i\eta(a+a^\dagger)}\rho = e^{\pm i\bar{\eta}\hat{x}}\rho \to e^{\pm i\bar{\eta}x}\left(1 \mp \frac{\bar{\eta}}{2}\partial_p\right)w(x,p), \qquad \rho e^{\pm i\eta(a+a^\dagger)} = \rho e^{\pm i\bar{\eta}\hat{x}} \to e^{\pm i\bar{\eta}x}\left(1 \pm \frac{\bar{\eta}}{2}\partial_p\right)w(x,p).$$

where $\hat{x} = \frac{1}{\sqrt{2}}(a+a^\dagger)$ and we introduced the scaled Lamb-Dicke factor $\bar{\eta} = \sqrt{2}\eta$. Note that this approximation is weaker than the usual Lamb-Dicke approximation. We can now perform second order perturbation theory in the terms of order $\bar{\eta}$, and derive a recursion relation in order to describe the change in the Wigner function from the n-th to the $(n+1)$-th spectroscopy pulse. Turning the recursion relation into a differential equation yields a Fokker-Planck equation for the dynamics of the normal mode

$$\partial_s W(x,p,s) = \left[-\left(\partial_x d_x + \partial_p d_p\right) + \frac{1}{2}\left(\partial_{xx}D_{xx} + \partial_{pp}D_{pp} + 2\partial_{xp}D_{xp}\right)\right]W(x,p,s), \tag{2}$$

where s is the spectroscopy time (dimensionless in units of spectroscopy pulse length τ). The drift and diffusion coefficients are

$$d_x = -\frac{\eta\Omega}{\sqrt{2}}\int_0^\tau \mathrm{d}t \sin(\omega_{\mathrm{m}}t)\langle\sigma_y(t)\rangle, \tag{3}$$

$$d_p = \frac{\eta\Omega}{\sqrt{2}}\int_0^\tau \mathrm{d}t \cos(\omega_{\mathrm{m}}t)\langle\sigma_y(t)\rangle, \tag{4}$$

$$D_{xx} = (\eta\Omega)^2\int_0^\tau \mathrm{d}t\int_0^t \mathrm{d}t' \sin(\omega_{\mathrm{m}}t)\sin(\omega_{\mathrm{m}}t')\mathrm{Re}\left(\langle\sigma_y(t)\sigma_y(t')\rangle\right) - d_x^2, \tag{5}$$

$$D_{pp} = (\eta\Omega)^2\int_0^\tau \mathrm{d}t\int_0^t \mathrm{d}t' \cos(\omega_{\mathrm{m}}t)\cos(\omega_{\mathrm{m}}t')\mathrm{Re}\left(\langle\sigma_y(t)\sigma_y(t')\rangle\right) - d_p^2, \tag{6}$$

$$D_{xp} = -(\eta\Omega)^2\int_0^\tau \mathrm{d}t\int_0^t \mathrm{d}t' \frac{1}{2}\left[\sin(\omega_{\mathrm{m}}t)\cos(\omega_{\mathrm{m}}t') + \sin(\omega_{\mathrm{m}}t')\cos(\omega_{\mathrm{m}}t)\right]\mathrm{Re}\left(\langle\sigma_y(t)\sigma_y(t')\rangle\right) - d_x d_p. \tag{7}$$

The mean values can be evaluated from the Bloch equations,

$$\frac{\mathrm{d}}{\mathrm{d}t}\langle\vec{\sigma}(t)\rangle = M\langle\vec{\sigma}(t)\rangle + \Gamma\vec{m}, \qquad M = \begin{pmatrix} -\Gamma/2 & \Delta_{\mathrm{dop}} & 0 \\ -\Delta_{\mathrm{dop}} & -\Gamma/2 & -\Omega \\ 0 & \Omega & -\Gamma \end{pmatrix}, \qquad \vec{m} = -\begin{pmatrix} 0 \\ 0 \\ 1 \end{pmatrix},$$

where $\vec{\sigma} = (\sigma_x, \sigma_y, \sigma_z)$ is a vector containing the Pauli matrices, and $\Delta_{\mathrm{dop}}(p) = \Delta - \bar{\eta}\omega_{\mathrm{m}}p$ is a Doppler shifted detuning. For the ion being in its ground state at the beginning of each spectroscopy pulse we

have to use the initial condition $\langle\vec{\sigma}(0)\rangle = \vec{m}$, such that the solution to the Bloch equations is $\langle\vec{\sigma}(t)\rangle = \left[e^{Mt}\left(1+\Gamma M^{-1}\right)-\Gamma M^{-1}\right]\vec{m}$. The two-time correlation function can be evaluated using the the quantum regression theorem

$$\frac{\mathrm{d}}{\mathrm{d}t'}\langle\vec{\sigma}(t+t')\sigma_y(t)\rangle = M\langle\vec{\sigma}(t+t')\sigma_y(t)\rangle + \langle\sigma_y(t)\rangle\Gamma\vec{m}, \qquad \langle\vec{\sigma}(t)\sigma_y(t)\rangle = \begin{pmatrix} i\langle\sigma_z(t)\rangle \\ 1 \\ -i\langle\sigma_x(t)\rangle \end{pmatrix},$$

where the latter has to be used as initial condition for the first equation, and we use the notation $\langle\vec{\sigma}(t+t')\sigma_y(t)\rangle_j = \langle\sigma_j(t+t')\sigma_y(t)\rangle$ with $j = x, y, z$. The solution is $\langle\vec{\sigma}(t+t')\sigma_y(t)\rangle = e^{Mt'}\left(\langle\vec{\sigma}(t)\sigma_y(t)\rangle + \langle\sigma_y(t)\rangle\Gamma M^{-1}\vec{m}\right) - \langle\sigma_y(t)\rangle\Gamma M^{-1}\vec{m}$.

The solutions for $\langle\sigma_y(t)\rangle$ and $\langle\sigma_y(t)\sigma_y(t')\rangle$ can be inserted into the expressions for the drift and diffusion coefficients. The remaining time integrals can in principle be evaluated analytically. Note that due to the Doppler shift in the detuning Δ_{dop} all drift and diffusion coefficients in Eq. (2) have in principle a nonlinear dependence on the momentum variable p. However, in first order of Lamb-Dicke expansion only the drift in momentum d_p is Doppler shifted such that we can approximate

$$d_p(p) = d_p(0) + \frac{\partial d_p}{\partial\Delta_{\mathrm{dop}}}\frac{\partial\Delta_{\mathrm{dop}}}{\partial p}p = d_p - gp, \qquad g = \sqrt{2}\eta\omega_{\mathrm{m}}\frac{\partial d_p}{\partial\Delta}. \tag{8}$$

g thus describes a Doppler shift induced (anti)damping rate for positive (negative) values of g, that is for red (blue) detuning from resonance. All other drift and diffusion coefficients show a weaker dependence on the momentum variable of higher order in the Lamb-Dicke parameter, such that we can neglect their dependence on p and set $\Delta_{\mathrm{dop}} = \Delta$ when evaluating Eqs. (3)-(7). As a result all drift and diffusion coefficients will be even functions in the detuning, and g will be an odd function.

Exact solution to diffusion equation — With the linear approximation (8) for the Doppler shift the Fokker-Planck equation (2) describes a Gaussian dynamics. When the normal mode is prepared initially in its ground state, the state will be fully characterized by its first and second moments at all subsequent times. These are conveniently collected in the displacement vector $\vec{r} = \langle\vec{R}\rangle$ and the covariance matrix $\gamma_{ij} = \langle R_iR_j + R_jR_i\rangle - 2r_ir_j$ where $\vec{R} = (\hat{x}, \hat{p})^T$ and $i, j = 1, 2$. Solving the Fokker-Planck with initial conditions $\vec{r} = 0$ and $\gamma = \mathbb{1}$ (the 2×2 identity matrix) one finds

$$\vec{r}(s) = \begin{pmatrix} d_x s \\ \frac{1-e^{-gs}}{g}d_p \end{pmatrix}, \qquad \gamma(s) = \begin{pmatrix} 1+2D_{xx}s & \frac{1-e^{-gs}}{g}2D_{xp} \\ \frac{1-e^{-gs}}{g}2D_{xp} & e^{-2gs}+\frac{1-e^{-2gs}}{2g}2D_{pp} \end{pmatrix}. \tag{9}$$

The probability to excite the ion from its ground state after a spectroscopy time s follows as

$$P(s) = 1 - \left|\frac{\mathbb{1}+\gamma(s)}{2}\right|^{-1/2}\exp\left[-\vec{r}(s)^T(\mathbb{1}+\gamma(s))^{-1}\vec{r}(s)\right], \tag{10}$$

from which the shift Δf can be extracted numerically using the two point sampling method.

Estimate for one dimension — In order to arrive at a simple physical picture of the Doppler induced shift we neglect the small drift and diffusion in position, that is, we set $d_x = D_{xx} = D_{xp} = 0$. These coefficients will be smaller than the respective ones for the momentum by at least a factor $(\omega_{\mathrm{m}}\tau)$ (trap frequency times pulse length). Thus, we effectively reduce our description to a one dimensional drift and diffusion process for the momentum. The mean momentum $\langle\hat{p}\rangle = r_2$ and its variance $v_p = \langle p^2\rangle - \langle p\rangle^2 = \gamma_{22}/2$ evolve, according to Eq. (9), as

$$\langle p(s)\rangle = \frac{1-e^{-gs}}{g}d \simeq ds - \frac{ds^2}{2}g, \qquad v_p(s) = e^{-2gs} + \frac{1-e^{-2gs}}{g}D_{pp} \simeq 1 + 2(D_{pp}-g)s.$$

The approximations represent first order Taylor expansions in the Doppler shift induced damping/heating rate g and diffusion D_{pp}. Note that, in leading order, the Doppler shift contributes to the variance *linearly* and to the mean momentum *quadratically* in s. In this order of s, and for the parameter regime considered here, the diffusion D_{pp} will make a negligible contribution as compared to g. In the following we will therefore set $D_{pp} = 0$. With the current approximation the excitation probability (10) becomes

$$P(s) = 1 - \left[\frac{2}{1+v_p(s)}\right]^{1/2} \exp\left[-\frac{\langle p(s)\rangle^2}{1+v_p(s)}\right] \simeq P_0(s) + \delta P(s),$$

where

$$P_0(s) = 1 - \exp\left[-\frac{d_p^2 s^2}{2}\right], \qquad \delta P(s) = \exp\left[-\frac{d_p^2 s^2}{2}\right]\frac{gs}{2},$$

are, respectively, the excitation probability without Doppler shift and the first order correction in g. $P_0(s)$ will be an entirely even function in the detuning, while the small correction $\delta P(s)$ is odd in the detuning. $P_0(s)$ reproduces the scaling with the number of spectroscopy pulses and the Lamb-Dicke factor as stated in the main text. For a given spectroscopy time s the shift Δf of the center of $P(s)$ away from $\Delta = 0$, as determined by the two point sampling method, therefore is

$$2\pi\Delta f = \frac{\delta P(s)}{\frac{\partial P_0(s)}{\partial\Delta}} = \frac{g}{2d_p s\frac{\partial d_p}{\partial\Delta}} = \frac{\eta\omega_{\mathrm{m}}}{\sqrt{2}d_p s},$$

where we used the definition of g in Eq. (8). If the two point sampling method is applied at a fixed motional excitation probability $p_{\mathrm{l,r}}$ the detuning Δ (and therefore the drift per pulse d_p) is effectively tied to the spectroscopy time such that (to zeroth order in g) $p_{\mathrm{l,r}} = P_0(s)$ or, equivalently, $d_p s = \sqrt{-2\log(1-p_{\mathrm{l,r}})}$. Overall the shift, as measured in the two point sampling method with signal amplitude $p_{\mathrm{l,r}}$ is roughly independent from the spectroscopy time, and given by

$$2\pi\Delta f = \frac{\eta\omega_{\mathrm{m}}}{2}\left[\log\left(\frac{1}{1-p_{\mathrm{l,r}}}\right)\right]^{-1/2}, \tag{11}$$

as stated in the main text.

Supplementary Note 3

Numerical Simulations

Numerical simulations have been performed using QuTiP [51]. For this, the Master equation Eq. 1 is implemented in 1st order Lamb-Dicke approximation. To include the effect of Zeeman broadening and optical pumping, the master equation (1) is expanded into a system containing eight electronic levels. Up to 20 motional levels of the normal mode are taken into account. The effect of recoil from spontaneous emission on the final spectroscopy signal has been found to be negligible at the 1 kHz level and has therefore been omitted. Using the experimentally determined parameters for the magnetic field, pulse length and Rabi frequency, we simulate the resonance curve as shown in Fig. 3a, which agrees well with the experimental data. The Rabi frequency of the spectroscopy laser is found by simultaneous fitting of simulated excitation signals as a function of the number of pulses to data of the observed signal with and without repumper. Fit parameters are the Rabi frequency, a signal offset and an amplitude reduction factor arising from experimental imperfections. The signal strength as a function of the number of absorbed photons are extracted from the simulated $^2P_{1/2}$ population of the signal with repumper. An excitation signal of 0.5 corresponding to a SNR of one is reached after 40 spectroscopy/repump pulses. The integrated $^2P_{1/2}$-state population corresponds to 9.8(1.2) absorbed photons. From simulated resonances curves similar to Fig. 3a using the experimentally calibrated Rabi frequency $\Omega = 2\pi \times 5.6$ MHz and 70 excitation pulses with a pulse length of $\tau = 125$ ns, a lineshape shift of 151(20) kHz can be extracted for the two-point sampling technique, assuming conservatively estimated fluctuations of the detection signal of ± 0.1.

Supplementary References

[50] D. J. Berkeland, J. D. Miller, J. C. Bergquist, W. M. Itano, and D. J. Wineland, *Minimization of ion micromotion in a Paul trap*, J. Appl. Phys. **83**, 5025–5033 (1998).

[51] J. Johansson, P. Nation, and F. Nori, *QuTiP 2: A Python framework for the dynamics of open quantum systems*, Computer Physics Communications **184**, 1234–1240 (2013).